Validation of Satellite Retrievals of Cloud Microphysics and Liquid Water Path Using Observations from FIRE

Q. Han,* W. Rossow,[†] R. Welch,* A. White,** AND J. Chou*

*Institute of Atmospheric Sciences, South Dakota School of Mines and Technology, Rapid City, South Dakota
[†]NASA/Goddard Institute for Space Studies, New York, New York
**NOAA/ERL/ETL, Boulder, Colorado

ABSTRACT

Cloud effective radii (r_e) and cloud liquid water path (LWP) are derived from ISCCP spatially sampled satellite data and validated with ground-based pyranometer and microwave radiometer measurements taken on San Nicolas Island during the 1987 FIRE IFO. Values of r_e derived from the ISCCP data are also compared to values retrieved by a hybrid method that uses the combination of LWP derived from microwave measurement and optical thickness derived from GOES data. The results show that there is significant variability in cloud properties over a 100 km × 80 km area and that the values at San Nicolas Island are not necessarily representative of the surrounding cloud field. On the other hand, even though there were large spatial variations in optical depth, the r_e values remained relatively constant (with $\sigma \leqslant$ 2–3 μm in most cases) in the marine stratocumulus. Furthermore, values of r_e derived from the upper portion of the cloud generally are representative of the entire stratiform cloud. When LWP values are less than 100 g m^{-2}, then LWP values derived from ISCCP data agree well with those values estimated from ground-based microwave measurements. In most cases LWP differences were less than 20 g m^{-2}. However, when LWP values become large (e.g., $\geqslant$200 g m^{-2}), then relative differences may be as large as 50%–100%. There are two reasons for this discrepancy in the large LWP clouds: 1) larger vertical inhomogeneities in precipitating clouds and 2) sampling errors on days of high spatial variability of cloud optical thicknesses. Variations of r_e in stratiform clouds may indicate drizzle: clouds with droplet sizes larger than 15 μm appear to be associated with drizzling, while those less than 10 μm are indicative of nonprecipitating clouds. Differences in r_e values between the GOES and ISCCP datasets are found to be 0.16 $\pm$ 0.98 μm.

1. Introduction

Clouds are one of the largest sources of uncertainty in climate change studies. A particular limitation in our understanding of the climate is the uncertainty in cloud property–radiative feedbacks (Rossow et al. 1989). Cloud optical thickness, microphysics, and liquid water content are among the parameters that are important feedback mechanisms (e.g., Platt 1989; Somerville and Remer 1984). Satellite observations of these cloud properties are crucial for improving our knowledge in this field. As the first program of the World Climate Research Programme, the International Satellite Cloud Climatology Project (ISCCP) supplies global information about cloud optical thickness and cloud-top height (Rossow and Schiffer 1991). A recent study has developed a method to extend the ISCCP analysis to retrieve cloud droplet radii and, combined with the modified cloud optical thickness retrievals, to produce cloud liquid water path information on a near-global scale (Han 1992; Han et al. 1994).

Extensive efforts are being made to validate satellite retrievals using data from the First ISCCP Regional Experiment (FIRE) field campaigns (e.g., Nakajima et al. 1991). Due to the specific time of the satellite overpasses (typically once per day), the limited regions in which in situ aircraft measurements were taken, and the highly variable (temporally and spatially) characteristics of cloud properties, there are very limited coincident sets of satellite observations and in situ measurements. These difficulties are increased somewhat for comparisons with the ISCCP datasets that are sampled at 3-h, 30-km intervals; however, this sampling does capture an accurate statistical measure of the cloud variability (Seze and Rossow 1991). A hybrid method recently has been developed by Minnis et al. (1992) to study diurnal variations of cloud microphysics and liquid water path. They combined satellite (GOES) observed cloud optical thicknesses and ground-based microwave observations of cloud liquid water path (LWP) to retrieve cloud droplet radii in stratocumulus. These results, acquired for 1–18 July 1987 over San Nicolas Island, have smaller spatial (8 km) and tem-

Corresponding author address: Dr. Qingyuan Han, Institute of Atmospheric Sciences, South Dakota School of Mines and Technology, 501 E. St. Joseph St., Rapid City, SD 57701-3995.

poral (hourly) sampling intervals than those available using the ISCCP. Surface observations have even higher time-sampling frequencies but only at one location. We attempt to overcome the problems associated with these different sampling characteristics by comparing aircraft and ground observations with two different satellite sensors. This paper presents comparisons of 1) cloud liquid water paths retrieved by ISCCP and ground-based microwave observations and 2) cloud microphysics results retrieved by ISCCP and GOES. Section 2 describes the ground observational data and satellite observations used in this study. Section 3 outlines the methodology used to retrieve cloud droplet radius and liquid water path. Section 4 presents the results, and section 5 concludes.

2. Data

a. Ground observations

Surface-based measurements using a pyranometer and a microwave radiometer were obtained on the northwest tip of San Nicolas Island (33°16′37″N, 199°34′34″W), located approximately 100 km southwest of Los Angeles, California (Fig. 1). Extended time observations (ETO) were made on the island from March to October 1987 (Fairall et al. 1990). The sensors used for the ETO were mounted on a small scaffold, and the data acquisition equipment was located in a nearby trailer. The sensors were sampled about once per second. Half-hour means and standard deviations were stored on a Campbell Model 21× data logger. This data then was periodically transferred to The Pennsylvania State University via telephone lines using standard modems.

The site chosen for the ETO experiences marine airflow most of the time. Therefore, the instruments were chosen based on their ability to withstand several months of exposure to the harsh marine environment. The Eppley PSP pyranometer has a standard Schott glass dome that is transparent in the 0.28 to 3 μm wavelength range. Two of these pyranometers were used to measure solar irradiance. One sensor was used continuously and provided the basic measurements, while the other sensor, which was kept covered except for occasional comparison periods, served to monitor the possible deterioration of the continuously exposed sensor. The maximum disagreement between the two pyranometers was no more than a few percent (Fairall et al. 1990).

The intensive field operations (IFO) phase of FIRE lasted from 29 June to 19 July 1987. A complete description of the FIRE IFO is given by Albrecht et al. (1988).

The NOAA/ETL microwave radiometer (Hogg et al. 1983) uses three channels for the simultaneous measurement of atmospheric water vapor and liquid water: a wavelength of 1.46 cm (20.6 GHz) is sensitive pri-

marily to water vapor, a wavelength of 0.95 cm (31.65 GHz) is sensitive primarily to liquid water, and a wavelength of 0.33 cm (90.0 GHz) is sensitive to both vapor and liquid. The three radiometers are coupled into a common antenna system with concentric beams of equal 2.5-degree width. A motor is used to steer the antenna system, but the antenna beams were directed only to the zenith for collecting data during the FIRE IFO. Radiometer data were averaged over 1-min intervals. In order to compare with GOES observations, the microwave data used in this study is limited to 1-hour average values.

Due to uncertainties in the retrieval of water vapor absorption at 0.33 cm, data from the 1.46- and 0.95 cm channels were used to retrieve vapor and liquid path values. The statistical retrieval technique is described in Hogg et al. (1983). The estimated uncertainty in the liquid path measurement is 20% (Fairall et al. 1990). Snider (1988) compared radiometric water vapor retrievals with radiosonde data over extended periods and found the rms differences between the two independent measurements to be ≤0.8 mm.

b. Satellite data

The dataset used to retrieve cloud droplet size and optical thickness is the ISCCP analysis (Rossow and Schiffer 1991) at individual pixel level. These CX data are a combination of ISCCP B3 data (Schiffer and Rossow 1983) and the cloud detection and radiative model analysis results that describe cloud and surface properties at the original B3 image resolution. Specifically, we use the results from Advanced Very High Resolution Radiometer (AVHRR) observations, which contain the radiances of all five AVHRR spectral channels (0.57–0.69, 0.72–0.98, 3.53–3.93, 10.30–11.30, and 11.50–12.50 μm for channels 1 to 5, respectively), surface reflectances and temperatures, a cloud detection flag, and the retrieved cloud optical thicknesses and cloud-top temperatures/pressures. The atmospheric temperature and humidity profiles needed in our retrieval are taken from the NOAA TIROS Operational Vertical Sounder (TOVS) product (Rossow et al. 1991). Cloud droplet effective radius r_e is retrieved, and the original ISCCP values[1] of cloud optical thickness τ are adjusted for consistency. Combining r_e and τ, cloud LWP can be derived from

$$\text{LWP} = 4/(3Q_{\text{ext}})r_e\tau\rho_w, \qquad (1)$$

where Q_{ext} is the average extinction efficiency over the droplet size distribution calculated from Mie scattering theory and ρ_w is the density of water. The Mie calculation shows that, at $\lambda = 0.65$ μm, $Q_{\text{ext}} = 2.16, 2.10,$

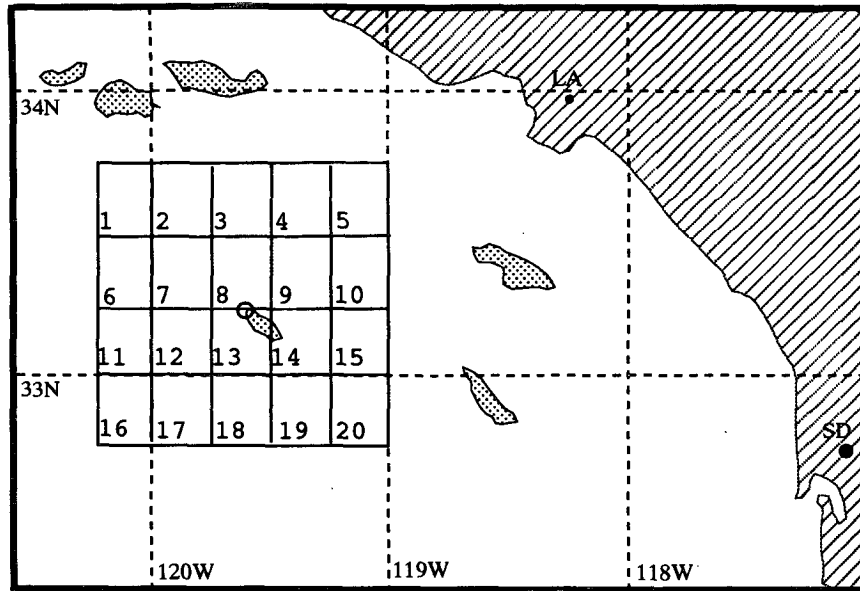[1] ISCCP optical thicknesses are retrieved assuming an effective droplet radius of 10 μm (Rossow et al. 1991).

FIG. 1. Location of San Nicolas Island and grid boxes used in the text.

2.08, 2.06, and 2.05, for r_e = 5, 10, 15, 20, and 30 μm, respectively. Therefore, using average values of Q_{ext} causes errors less than 3%. Note that this analysis retrieves only effective radius from the tops of clouds; therefore, the results may overestimate or underestimate LWP if r_e is not a good approximation of the vertically averaged effective radius over the whole cloud layer (Nakajima et al. 1991).

A hybrid method has been developed by Minnis et al. (1992) to study diurnal variations of cloud microphysics and liquid water path. They combined satellite (GOES) observed cloud optical thickness and ground-based microwave observation of cloud liquid water path (LWP) to retrieve cloud droplet radii in stratocumulus. More frequent results (at a maximum of once per hour during daytime) of cloud droplet radii and cloud optical thickness were acquired during 1–18 July 1987 at San Nicolas Island. This dataset offers more complete temporal observations and provides another basis for validation of satellite retrievals.

3. ISCCP LWP and cloud droplet radius

The ISCCP LWP computation is based on the results of cloud optical thickness and particle size retrievals. Cloud optical thickness is obtained from the visible (0.6 μm) wavelength band (Rossow and Schiffer 1991). To retrieve cloud droplet size, we use AVHRR channel 4 radiances (10.5 μm) to determine the thermal emission contribution to the channel 3 radiances and the channel 1 (0.6 μm) radiances to retrieve the optical thickness. A radiative transfer model that includes all major absorbing gases and cloud scattering/absorption is used to compute synthetic radiances for the specific

satellite viewing geometry. The model results have been validated against clear-sky observations and are consistent with the observed radiance range under cloudy conditions. A method of estimating instrument noise and accounting for its effects on our analysis has also been developed (Han 1992). The sources of error in the retrieved cloud droplet sizes are 1) random error sources (instrument noise, uncertainty of atmospheric or surface input parameters); 2) calibration bias (difference between satellites, sensitivity drift with time for the same satellite); 3) radiative effects of horizontal inhomogeneity of clouds (broken cloudiness, morphology), which may be systematic for boundary layer clouds; 4) vertical inhomogeneity of clouds (multilayer clouds, droplet size change with altitude within a cloud), which may affect validation using in situ measurements; and 5) a positive bias caused by cirrus/aerosol contamination. The mean random errors are estimated to be $\sim$15%, and the bias to be about 1–2 μm, though for a specific pixel under different conditions (surface type, season, multilayer clouds, etc.) these values can be quite different (Han et al. 1994). Therefore, error sources and the range of their contributions are included for each retrieved cloud particle size. Comparison of retrieved droplet sizes between continental and maritime clouds is in good agreement with aircraft measurements described by other authors (Han et al. 1994). The estimated uncertainty of monthly mean values of r_e is 1–2 μm; however, validation is still so limited that validation studies must continue.

The radiative transfer model is described in detail in Han (1992). The model atmosphere is divided into 12 vertical, plane-parallel layers that are horizontally homogeneous. The temperature and humidity profiles are

prescribed from observations. The effects of non-plane-parallel radiative transfer in clouds are not dominant (cf. Kobayashi 1993) and are mitigated in our analysis by use of only near-nadir observations (see Han et al. 1994 for more discussion). The instrument "solar constants" for each satellite were calculated in the model using the instrument spectral response functions (Rossow et al. 1987) and the solar spectra [Thekaekara (1974) for channel 3 of AVHRR; Neckel and Labs (1984) for channels 1 and 2 of AVHRR]. Molecular scattering is included as Rayleigh scattering. Gaseous absorptions in the model atmosphere are from line absorptions by H_2O, CO_2, O_3, O_2, N_2O, and CH_4 and continuum absorptions by H_2O, O_3, and N_2. The atmosphere is considered to be in local thermal equilibrium, and thermal radiation is determined by the emissivity and the Planck function, which varies linearly over each model layer. The correlated k-distribution method (Lacis and Oinas 1991) is used to calculate gaseous absorption in a vertically inhomogeneous, scattering atmosphere. Surface reflectances are taken as Lambertian for land and ice-covered surfaces and as anisotropic (bidirectional) for water, following the model by Minnis and Harrison (1984).

Clouds are inserted into the atmospheric model as horizontally and vertically (within one model layer) homogeneous layers. Mie theory is used for calculating the wavelength-dependent phase function for liquid water spheres, and the adding–doubling method (Hansen and Travis 1974) is used to compute multiple scattering in clouds viewed from nadir, where scattering is azimuthly independent. Twelve Gauss points are used to account for varying solar zenith angles. The standard gamma distribution (Hansen 1971) is used for cloud droplet size distributions. This distribution agrees well with experimental data for low-level liquid water clouds, specifically stratus, altostratus, and fair weather cumulus (Hansen 1971). Note that throughout this paper we discuss the cloud optical thickness in terms of its value at 0.6 μm; however, the actual value is wavelength dependent in all model calculations.

To investigate the horizontal variations of cloud properties, 20 grid boxes covering roughly 100 km $\times$ 130 km are used (Fig. 1). Each box represents the area sampled by one satellite pixel (about 4 km in size) in the ISCCP dataset. The results of the ISCCP analysis are all at the original pixel level. The location of the original pixel (1 km $\times$ 4 km) in the 30 km $\times$ 30 km area is not known. The ground observation site at the northwest tip of San Nicolas Island (33.28°N, 119.58°W) falls on the border between the two closest ISCCP grid boxes (33.2°N, 119.6°W and 33.4°N, 119.6°W). To estimate the effect of location differences, three groups of ISCCP data in this area are used: 20 grid boxes (numbered 1–20 in Fig. 1), 6 grid boxes (numbers 7, 8, 9, 12, 13, 14 in Fig. 1), and 2 grid boxes (numbers 8 and 13 in Fig. 1). Average solar zenith angles in all three satellite datasets are used to deter-

mine the local time for comparison with surface observations.

Due to the near-nadir viewing limitation used in retrieving cloud droplet sizes from satellite (Han et al. 1994), ISCCP r_e, τ and LWP values are not available over San Nicolas Island for every day. For example, over the 20 grid box region, r_e, τ, and LWP values are retrieved by NOAA-10 data on 4, 5, 9, 14, 17, 18, 19, 23, and 28 July 1987 and by NOAA-9 data on 6, 7, 8, 15, 16, and 17 July 1987. For most of these days clouds are not present in all 20 grid boxes. A match between ISCCP results and ground observations occurs when r_e values are retrieved in the closest 2 grid box region.

4. Results and discussion

In this study we use the ISCCP results to obtain values of cloud optical thickness, τ, and effective droplet radius, r_e, from which we calculate values of cloud liquid water path, LWP. The values of LWP are validated by comparisons with two different inferences of LWP from surface-based measurements made at the same locations and times. We also compare with the collocated and contemporary analysis results of Minnis et al. (1992), who use satellite-derived values of τ, together with surface-based determinations of LWP, to calculate values of r_e. The mutual consistency of these four sets of results provides confidence in the satellite retrievals.

a. LWP

Since the LWP is simply proportional to the amount of absorption along the atmospheric path (Greenwald et al. 1993), microwave measurements of LWP are a NOAA operational product (Scofield 1991). In this study, LWP was derived by ground-based microwave observations during the FIRE II experiment at San Nicolas Island during 1–19 July 1987. There are nine matches with ISCCP results. Figure 2 is the comparison of LWP between satellite results (ISCCP) and ground-based microwave observation (GROUND). Results from six days agree very well (LWP differences less than 20 g m^{-2}); there is one overestimate (14 July, ISCCP $-$ GROUND $=$ 95 g m^{-2}), one significant underestimate (9 July, GROUND $-$ ISCCP $=$ 260 g m^{-2}), and one day with insufficient ground-based data (4 July). Possible reasons for the two anomalous cases (9 and 14 July) will be discussed in section 4c.

Figure 3 shows the intercomparison among results inferred from pyranometer observations (PYRANOMETER), microwave radiometer data (RADIOMETER), and ISCCP data (ISCCP) for July 1987. Comparisons between LWP derived from pyranometer data and microwave radiometer data have been shown by scatter plots in Fairall et al. (1990); the results show a 35% rms variability around the regression line between LWP values retrieved by pyranometer and radiometer
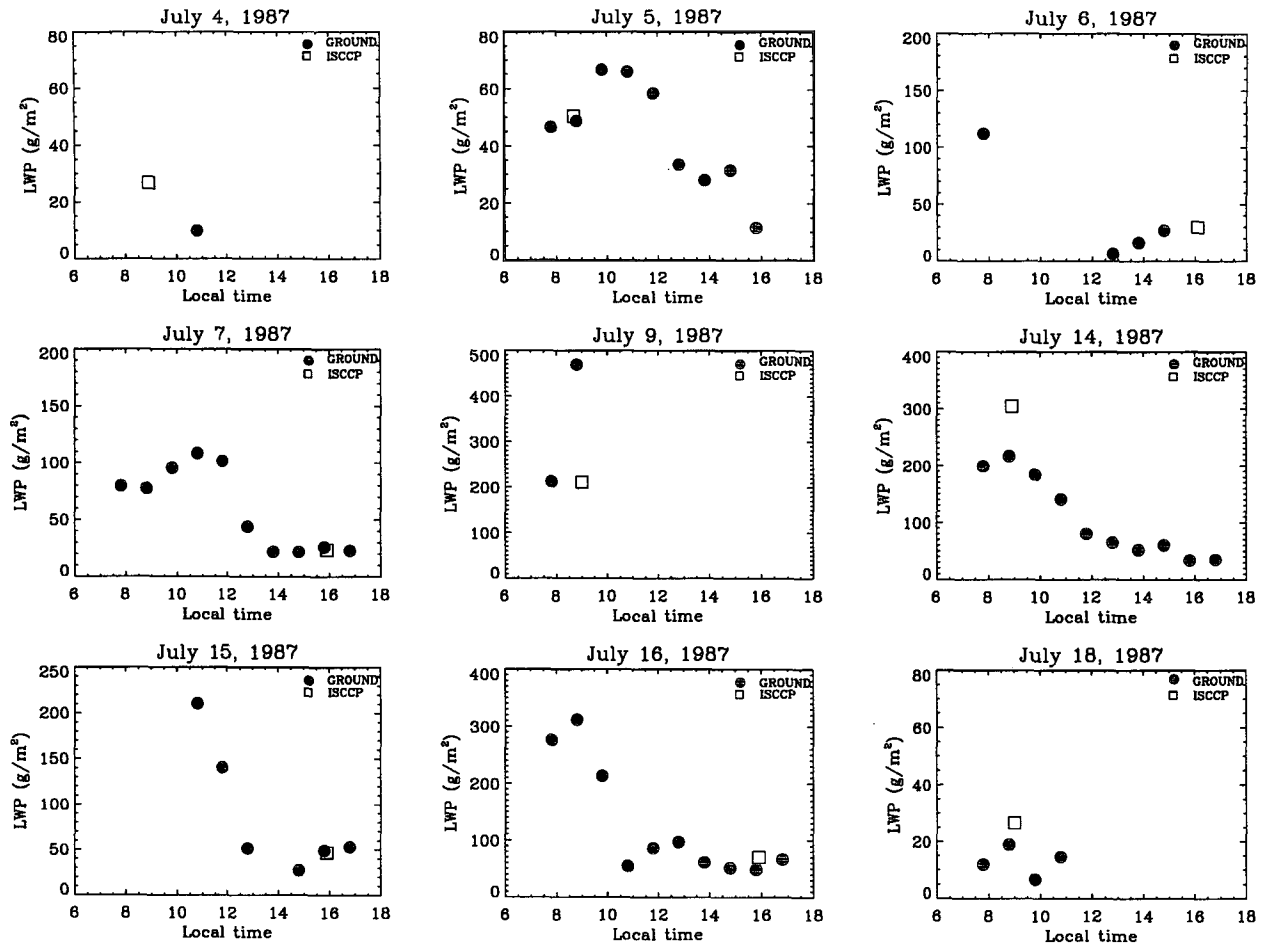
Fig. 2. Comparison of LWP values derived from ISCCP retrieval and microwave measurement.

data. However, the time sequence comparison shown in Fig. 3 gives the sense that these results closely follow the same variational trend. LWP values derived by ISCCP data show better agreement with results inferred from pyranometer data than with those from radiometer data for the 2 grid box case (Fig. 3). As the area coverage expands to 6 and then 20 grid boxes, significant spatial variations in LWP values derived from ISCCP data are found.

The time coverage of these three datasets is different: microwave radiometer data are for 1–19 July 1987; ISCCP retrieved results are for January, April, July, and October 1987; pyranometer observations are for February–October 1987. Hence, another intercomparison can be made between results inferred from ISCCP data and pyranometer observations for April and October 1987. Figures 4 and 5 show values of LWP for these intercomparisons. ISCCP data are sparse for April (Fig. 4). However, the agreement between ISCCP retrieval and pyranometer measurement is generally good (mean and standard deviation of differences of ISCCP-pyranometer: -14 ± 36 g m^{-2}) for the 2 grid box cases

available. For October (Fig. 5) results for seven days are in good agreement (mean and standard deviation of differences of ISCCP $-$ pyranometer: -6 ± 46 g m^{-2}); however, four days (14, 19, 25, 26) have significant discrepancies (mean and standard deviation of differences of ISCCP $-$ pyranometer: 205 ± 91 g m^{-2}), with ISCCP-retrieved LWP values being much larger than those measured by the pyranometer. One possible explanation is the effect of partial cloud cover over San Nicolas Island on those days. If the areal cloud cover is small, we might expect that the time and location mismatches between the satellite and surface observations would introduce larger differences than if the whole area were covered by relatively uniform overcast. Because the dome of the pyranometer has a hemispherical field of view and the AVHRR data used in this study has a near-nadir narrow field of view, a thick cloud covering a small part of overhead sky over San Nicolas Island region would be detected by AVHRR but may not block solar irradiance from reaching the pyranometer. Therefore, we checked the fractional cloud cover report from San Nicolas Island for
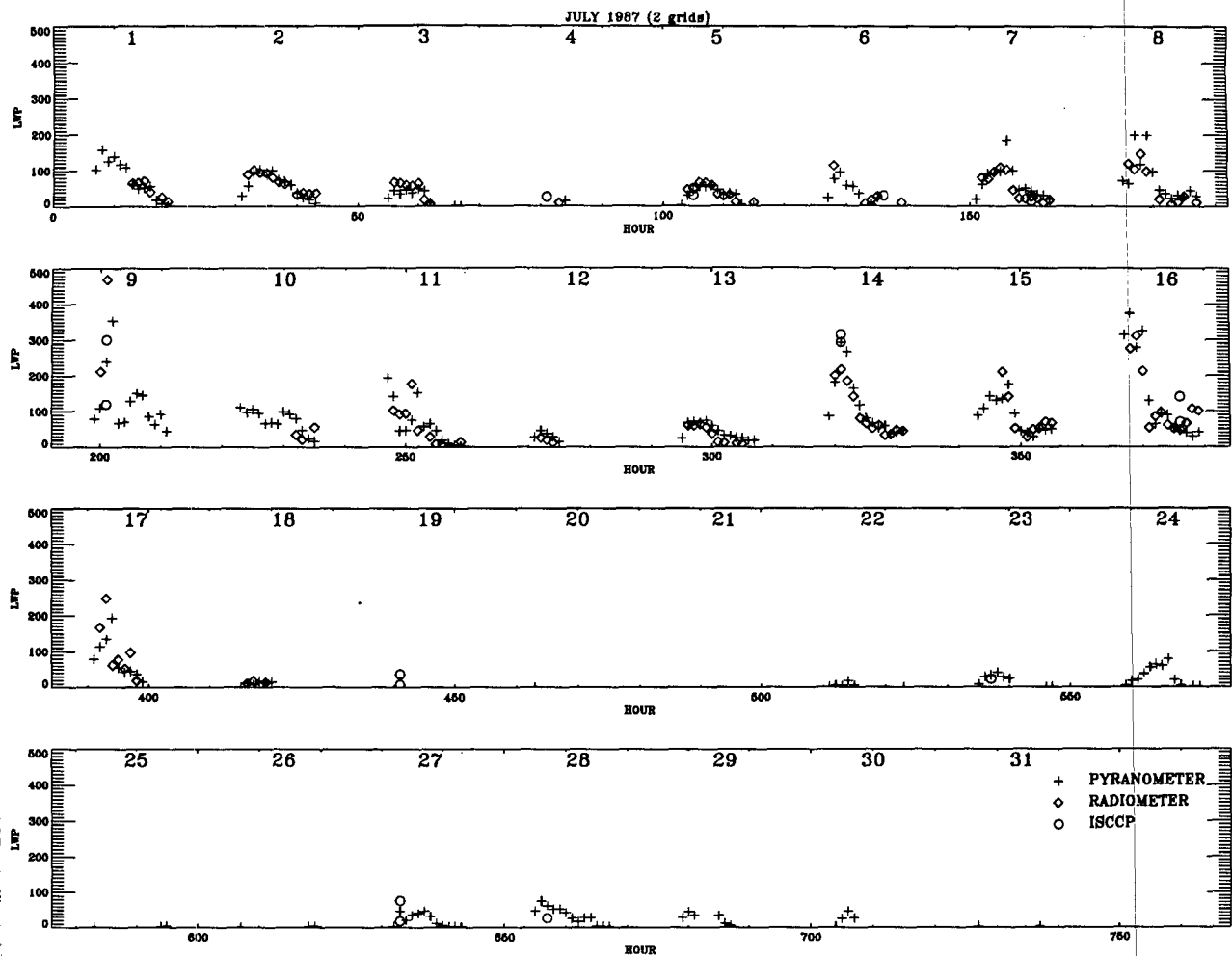
FIG. 3. Time sequence comparison of LWP in July 1987 derived from pyranometer, microwave radiometer, and 2-grid ISCCP data.

those days. According to the ceilometer data, discrepancies of 25 and 26 October may be explained by fractional cloud cover, because on these two days cloud cover was 9%–10%. But cloud cover was more than 90% for 14 and 19 October. Another possible explanation for these large errors is that the particular pixel used by the ISCCP sampling scheme was too far away from San Nicolas Island.

b. Horizontal homogeneity of cloud properties

Figure 6 shows mean values (μ) and standard deviations (σ) of cloud properties (optical thickness, effective radius, and liquid water path) derived from ISCCP data for the three different area coverages for days in July 1987. Similar results are found for April and October 1987. Most cases show less variation for small scales (2 or 6 grid boxes) than for large scales (20 grid boxes). This means that there is significant variation of cloud properties over a 100 km × 80 km area and that

the values at San Nicolas are not necessarily representative of the surrounding cloud field. Also shown in Fig. 6 are corresponding values of pyranometer and radiometer observations at the time of AVHRR overpasses. It is clear that, given the large range of variations, satellite and ground-observed values agree reasonably well with each other.

The other feature in Fig. 6 is that although there were large variations in optical depth the r_e values remain relatively constant (standard deviation $\sigma \leq 3$ μm for most cases) for marine stratus. This was also found by in situ aircraft observations (J. S. Foot 1994, personal communication) and was discussed by Han et al. (1994).

If we compare the spatial variations of LWP observed from satellites with the time variability of these same properties measured at one point on the surface, we find that they are similar in magnitude (cf. Cahalan et al. 1994). Thus, even though some differences between the surface and satellite results must be caused
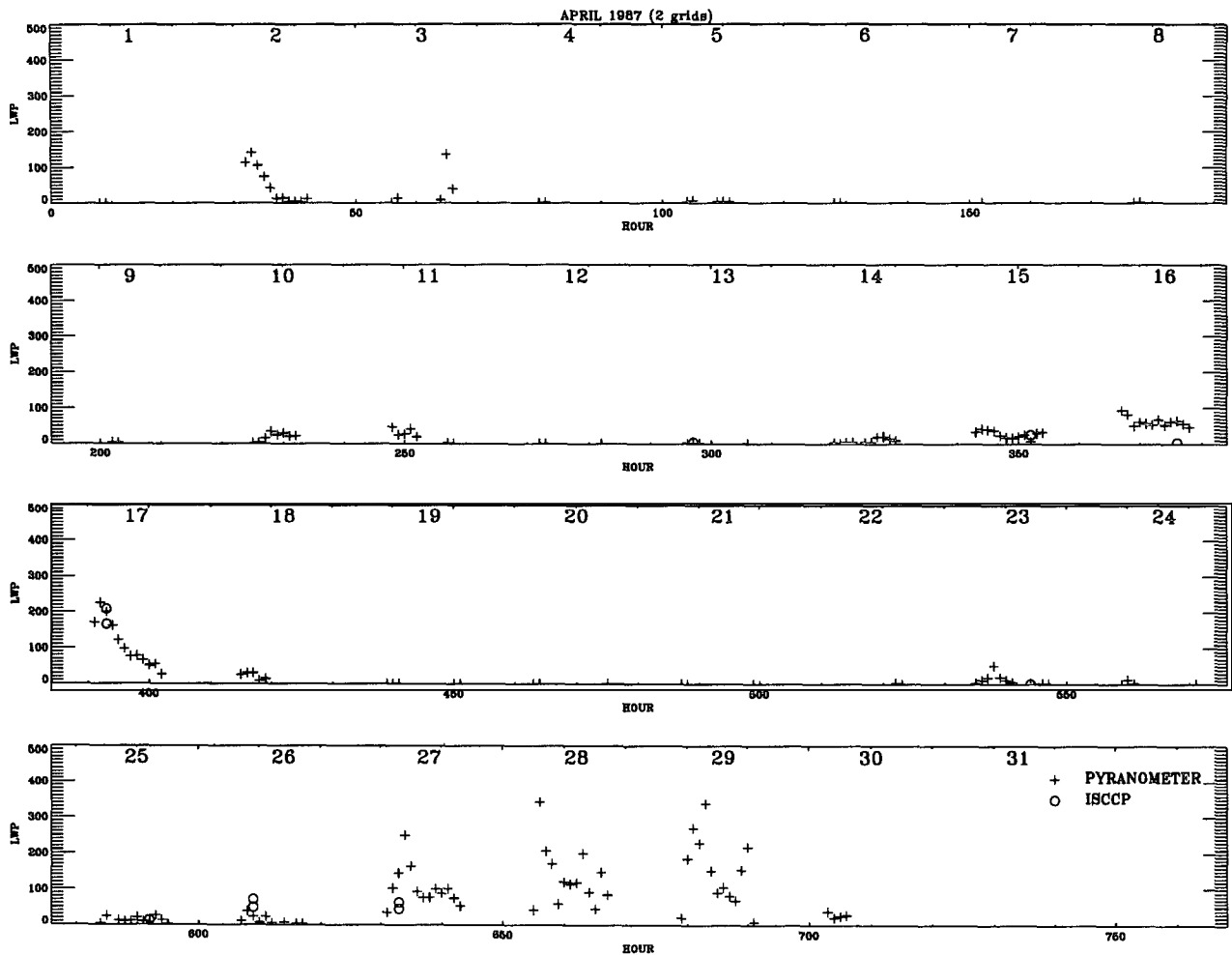
FIG. 4. Time sequence comparison of LWP in April 1987 derived from pyranometer and 2-grid ISCCP data.

by different sampling of the variable clouds, the statistics from the two observing systems (point with higher time resolution vs area with lower time resolution) are similar in character. Thus, the quantitative agreement between the satellite and surface values supports the estimates of the uncertainties in the satellite retrievals.

c. Droplet sizes

During the FIRE IFO, cloud effective droplet sizes were inferred by Minnis et al. (1992) using LWP values derived from ground-based microwave measurements and cloud optical thicknesses retrieved from the GOES satellite. Because the values of LWP and cloud optical thickness are properties of the total cloud layer, the inferred value of r_e represents an average droplet radius over the whole cloud layer. Comparing this inferred value of r_e with the value retrieved from ISCCP offers an estimate of how well the top-of-layer r_e represents the whole-layer-average r_e. We use cloud op-

tical thickness as an indication that these two data are derived from the same location.

Figures 7 and 8 show droplet sizes and cloud optical thickness for nine days in July 1987. In Fig. 7, results from in situ aircraft measurements by Rawlins and Foot (1990) (R&F in Fig. 7) and Nakajima et al. (1991) (N&K in Fig. 7) are also shown. The figure shows that droplet radius values for six days (days 5, 6, 7, 14, 15, 18) agree well with results obtained from the GOES data (mean and standard deviation of differences of ISCCP − GOES: 0.16 ± 0.98 μm). The good agreement for the 14 July case is surprising because the optical thickness from the ISCCP data is larger than the results from the GOES retrieval (Fig. 8). The large differences in optical thickness on that day suggests that the data from ISCCP may not coincide with those from GOES. A check of the horizontal variations of cloud properties on that day (Fig. 6) shows that the effective droplet radii were quite uniform over an area of about 100 km × 130 km² (10 ± 1 μm) but with large
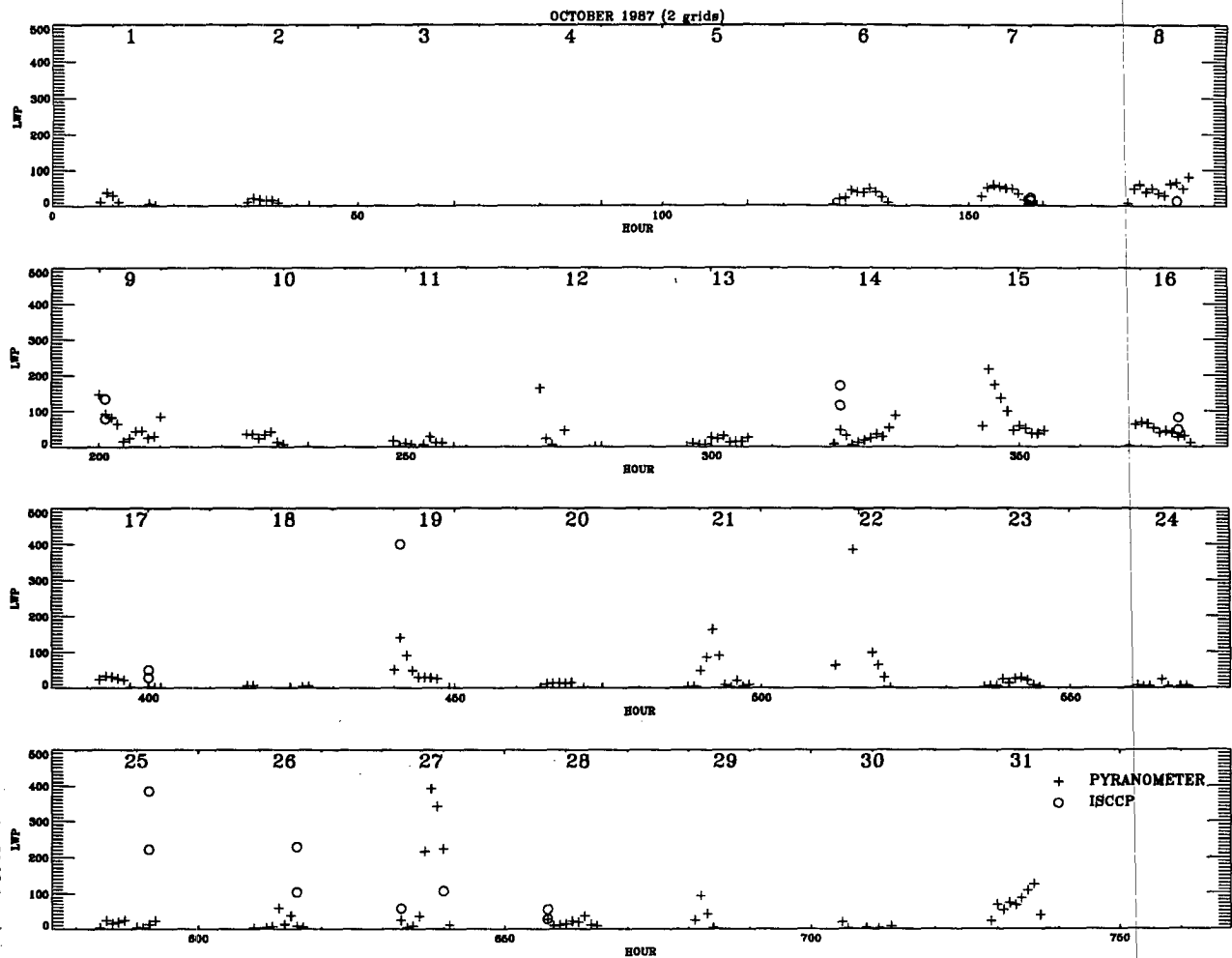
FIG. 5. Time sequence comparison of LWP in October 1987 derived from pyranometer and 2-grid ISCCP data.

variations of cloud optical thickness (38 ± 8) over the same region. Therefore, even though these two datasets may not have been completely collocated, which may cause the LWP difference (Fig. 2), there is good agreement between the r_e derived from GOES and ISCCP data; this is due to the homogeneity of cloud effective droplet radii on that day.

A significantly smaller value of r_e is obtained from the ISCCP retrieval, as compared to GOES data, on 9 July (Fig. 7); however, the cloud optical thickness differences between these two results are not significant (Fig. 8). This behavior is expected when cloud effective radius retrieved in the cloud-top layer is not representative of the whole cloud; such discrepancies are particularly significant if the cloud is drizzling. The underestimation of retrieved values of r_e comes from the fact that large precipitating particles are in the lower part of the cloud that cannot be sensed. The 16 July case also shows disagreement between the ISCCP and GOES retrievals. Since the ISCCP and GOES analyses both ob-

tain cloud optical thickness values from satellite-measured reflected sunlight, both their values will be insensitive to the presence of the much larger drizzle droplets, which scatter sunlight less efficiently than the smaller cloud droplets. However, since the ISCCP retrieval of r_e is based on sunlight reflected predominantly from near cloud top, whereas the GOES LWP value is based on surface microwave measurements which will include the drizzle drops, the retrieved values of r_e from GOES should be larger than the ISCCP values whenever drizzle is present. Large temporal fluctuations of effective radius are shown in Fig. 7. The ISCCP retrieval obtains a larger value of r_e as compared to the GOES data (Fig. 7), but the in situ aircraft measurements (Rawlins and Foot 1990; Nakajima et al. 1991) also show discrepancies with the GOES results. These differences may be caused by the highly variable nature of cloud properties on that day. Time and geographic differences during periods of high cloud property variability can be expected to confuse the intercomparisons.
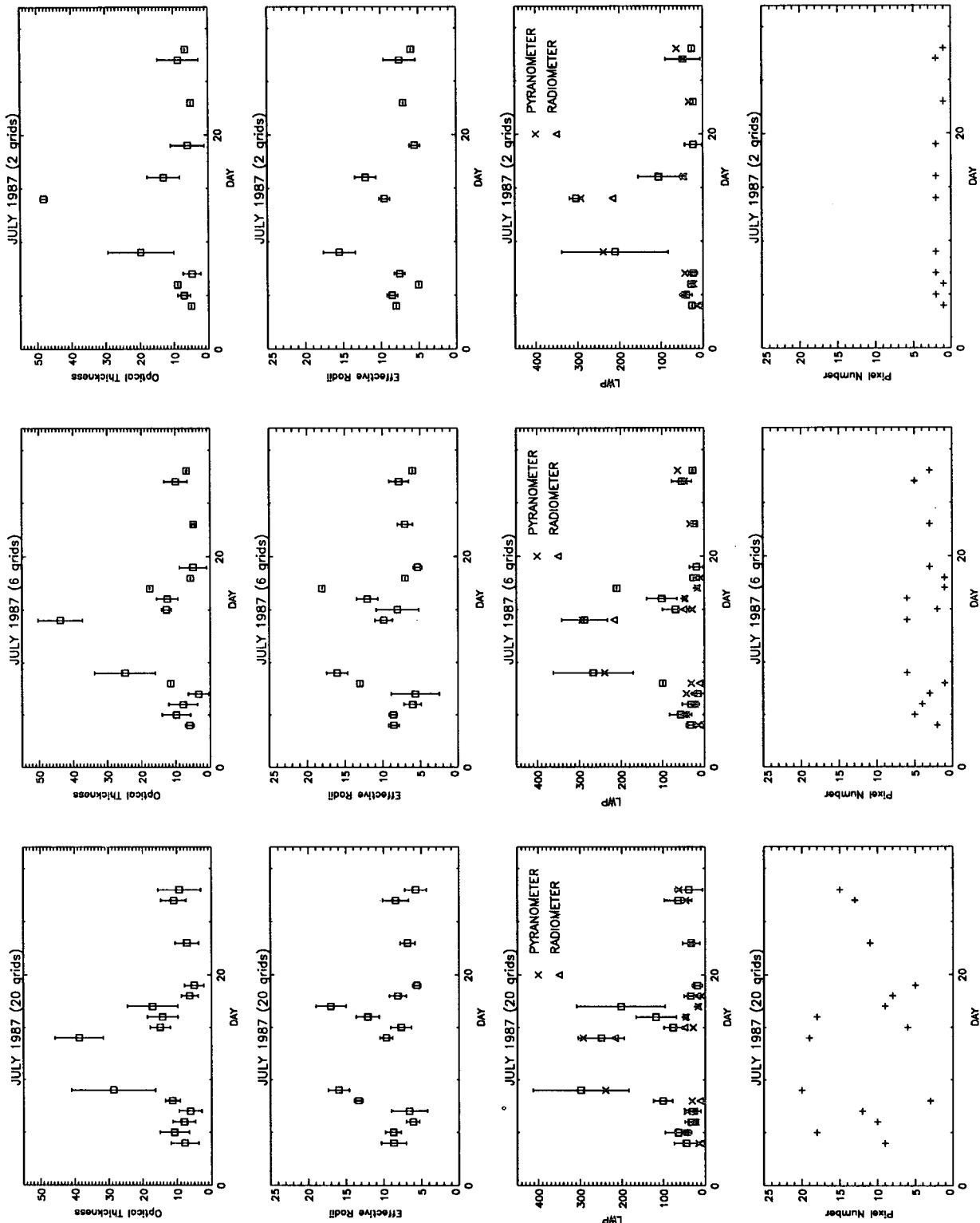
HAN ET AL.

FIG. 6. Mean values (μ) and standard deviations (σ) of cloud properties (optical thickness, effective radius, and liquid water path) derived from ISCCP data for the three different area coverages for days in July 1987.
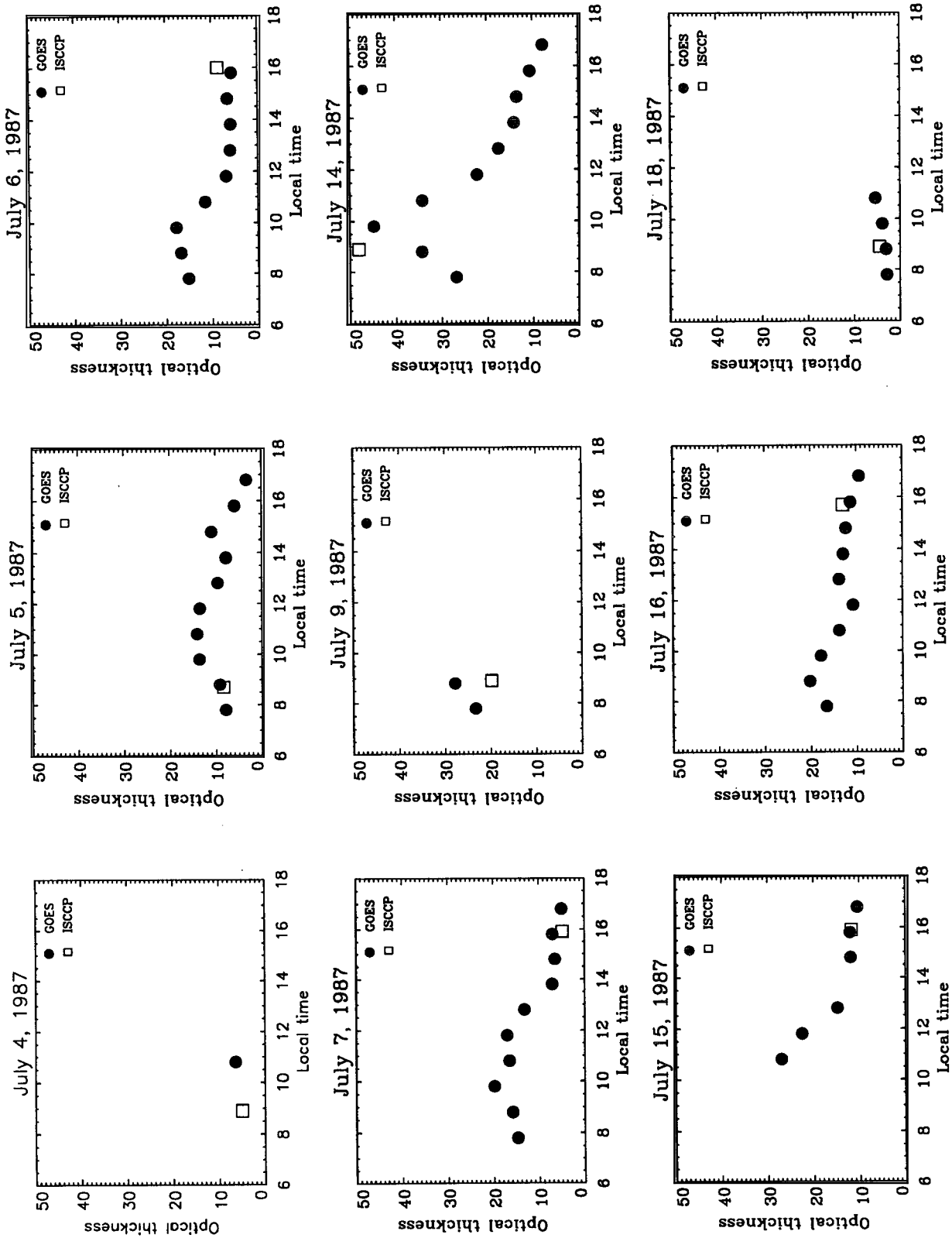
FIG. 7. Cloud droplet radii derived from ISCCP and GOES data. Results from in situ measurements by aircraft are also shown.

FIG. 8. Cloud optical thickness derived from ISCCP and GOES data.

Microwave studies of clouds (Liu and Curry 1993) suggest that precipitation occurs with high probability in clouds with LWP greater than 250–500 g m^{-2}. There are four days with LWP values greater than 100 g m^{-2}: 9, 14, 16, and 17 July (Fig. 6). According to ground observation records of microwave radiometer and ceilometer data, 9 and 17 July show drizzle features: sharp spikes in the radiometer records and sporadic near-ground cloud-base heights from ceilometer results. Satellite-retrieved cloud droplet radii for these two days are greater than 15 μm (Fig. 6). On the other hand, 14 July, with its LWP between the 9 and 17 July values, is a nonprecipitation day as indicated by cloud liquid water contents close to adiabatic (Albrecht et al. 1990). The droplet radius retrieved for this day is about 10 μm. The implication is that retrievals of effective particle size in stratocumulus with values of $r_e \geqslant 15$ μm may be indicative of drizzling. According to microwave radiometer and ceilometer records, 16 July is a possible, but not definite, drizzle day, and the retrieved droplet size is about 12 μm. This is consistent with the findings that $r_e = 14$ μm is the minimal radius needed for precipitation processes (Rosenfeld and Gutman 1994; Levi and Rosenfeld 1994).

5. Conclusions

Intercomparisons between satellite and ground-based cloud property retrievals (liquid water path, effective droplet radius) have been conducted using satellite data (ISCCP, GOES) and ground observations (pyranometer, microwave radiometer) during the FIRE IFO. The results show that r_e deduced from ISCCP data closely agree with the r_e by hybrid method (LWP derived from microwave measurement and cloud optical thickness retrieved from GOES data). This means that effective droplet radius (r_e) derived from the upper portion of the cloud generally is representative for the whole stratiform cloud. The LWP values derived from τ and r_e by ISCCP also agree well with those estimated from ground microwave measurements (with differences less than 10 g m^{-2}) when LWP values are less than 100 g m^{-2}. When LWP values become large (e.g., >200 g m^{-2}), the relative differences can be 50%–100% depending on the cloud conditions. There are two possible reasons for this discrepancy: 1) the r_e values retrieved from satellite data may be an underestimate of the average value for the whole cloud including drizzle; however, the retrieved droplet sizes may represent the cloud excluding drizzle, and 2) the difference is caused by the sampling (one 1 km × 4 km pixel out of about a 24 km × 30 km area) of ISCCP. Variations of r_e in stratiform clouds may be used to indicate drizzle: clouds with droplet sizes larger than 15 μm appear to be associated with drizzling and those less than 10 μm are indicative of nonprecipitating clouds. Yet validation is still very limited because few coincident in situ measurements are available. Further validation efforts are required.

REFERENCES

Albrecht, B. A., D. A. Randall, and S. Nicholls, 1988: Observations of marine stratocumulus clouds during FIRE. *Bull. Amer. Meteor. Soc.,* **69,** 618–626.

——, C. W. Fairall, D. W. Thomson, A. B. White, J. B. Snider, and W. H. Schubert, 1990: Surface based remote sensing of the observed and the adiabatic liquid water content of stratocumulus clouds. *Geophys. Res. Lett.,* **17,** 89–92.

Cahalan, R. F., W. Ridgway, W. J. Wiscombe, T. L. Bell, and J. B. Snider, 1994: The albedo of fractal stratocumulus clouds. *J. Atmos. Sci.,* **51,** 2434–2455.

Fairall, C. W., J. E. Hare, and J. B. Snider, 1990: An eight-month sample of marine stratocumulus cloud fraction, albedo, and integrated liquid water. *J. Climate,* **3,** 847–864.

Greenwald, T. J., G. L. Stephens, T. H. Vonder Haar, and D. L. Jackson, 1993: A physical retrieval of cloud liquid water over the global oceans using Special Sensor Microwave/Imager (SSM/I) observations. *J. Geophys. Res.,* **98,** 18 471–18 488.

Han, Q., 1992: Global survey of effective particle size in liquid water cloud by satellite observations. Ph.D. dissertation, Columbia University, 205 pp.

——, W. B. Rossow, and A. A. Lacis, 1994: Near-global survey of effective droplet radii in liquid water clouds using ISCCP data. *J. Climate,* **7,** 465–497.

Hansen, J. E., 1971: Multiple scattering of polarized light in planetary atmospheres. Part II. Sunlight reflected by terrestrial water clouds. *J. Atmos. Sci.,* **28,** 1400–1426.

——, and L. D. Travis, 1974: Light scattering in planetary atmospheres. *Space Sci. Rev.,* **16,** 527–610.

Hogg, D. C., F. O. Guiraud, J. B. Snider, M. T. Decker, and E. R. Westwater, 1983: A steerable dual-channel microwave radiometer for measurement of water vapor and liquid in the atmosphere. *J. Appl. Meteor.,* **22,** 789–806.

Kobayashi, T., 1993: Effects due to cloud geometry on biases in the albedo derived from radiance measurements. *J. Climate,* **6,** 120–128.

Lacis, A. A., and V. Oinas, 1991: A description of the correlated *k*-distribution method for modeling non-grey gaseous absorption, thermal emission, and multiple scattering in vertically inhomogeneous atmospheres. *J. Geophys. Res.,* **96,** 9027–9063.

Levi, Y., and D. Rosenfeld, 1994: Preliminary investigation of cloud top microphysical properties using satellite retrieved effective radius. *Proc. Sixth WMO Scientific Conf. on Weather Modification,* Paestum, Italy, World Meteor. Org., Rep. No. 22, 561–564.

Liu, G., and J. A. Curry, 1993: Determination of characteristic features of cloud liquid water from satellite microwave measurements. *J. Geophys. Res.,* **98,** 5069–5092.

Minnis, P., and E. F. Harrison, 1984: Diurnal variability of regional cloud and clear-sky radiative parameters derived from GOES data. Part II: November 1978 cloud distributions. *J. Climate Appl. Meteor.,* **23,** 1012–1031.

——, P. W. Heck, D. F. Young, C. W. Fairall, and J. B. Snider, 1992: Stratocumulus cloud properties derived from simultaneous satellite and island-based instrumentation during FIRE. *J. Appl. Meteor.,* **31,** 317–339.

Nakajima, T., M. D. King, and J. D. Spinhirne, 1991: Determination of the optical thickness and effective particle radius of clouds from reflected solar radiation measurements. Part II: Marine stratocumulus observations. *J. Atmos. Sci.,* **48,** 728–750.

Neckel, H., and D. Labs, 1984: The solar radiation between 3300 and 12500 Å. *Solar Phys.,* **90,** 205–258.

Platt, C. M. R., 1989: The role of cloud microphysics in high-cloud feedback effects on climate change. *Nature,* **341,** 428–429.

Rawlins, F., and J. S. Foot, 1990: Remotely sensed measurements of stratocumulus properties during FIRE using the C130 aircraft multi-channel radiometer. *J. Atmos. Sci.,* **47,** 2488–2503.

Rosenfeld, D., and G. Gutman, 1994: Retrieving microphysical properties of near the tops of potential rain clouds by multispectral analysis of AVHRR data. *J. Atmos. Sci.,* in press.

Rossow, W. B., and R. A. Schiffer, 1991: ISCCP cloud data products. *Bull. Amer. Meteor. Soc.,* **72,** 2–20.

——, E. Kinsella, A. Wolf, and L. Garder, 1987: International Satellite Cloud Climatology Project (ISCCP) description of reduced resolution radiance data. World Meteorological Organization Tech. Document WMO/TD-No. 58, 143 pp.

——, L. C. Garder, and A. A. Lacis, 1989: Global, seasonal cloud variations from satellite radiance measurements. Part I: Sensitivity of analysis. *J. Climate,* **2,** 419–458.

Schiffer, R. A., and W. B. Rossow, 1983: The International Satellite Cloud Climatology Project (ISCCP): The first project of the world climate research program. *Bull. Amer. Meteor. Soc.,* **64,** 779–784.

Scofield, R. A., 1991: Operational estimation of precipitation from satellite data. *Palaeogeogr., Palaeoclim., Palaeoecol.,* **90,** 79–86.

Seze, G., and W. B. Rossow, 1991: Effects of satellite data resolution on measuring the space–time variations of surfaces and clouds. *Int. J. Remote Sens.,* **12,** 921–952.

Snider, J. B., 1988: Verification of the accuracy of a network of water vapor radiometers. *Proc. IGARSS 88 Symp.,* Edinburgh, Scotland, IEEE, 19–20. [Available from IEEE, P.O. Box 1331, Piscataway, NJ, 08855-1331.]

Somerville, R. C., and L. A. Remer, 1984: Cloud optical thickness feedbacks in the CO_2 climate problem. *J. Geophys. Res.,* **89,** 9668–9672.

Thekaekara, M. P., 1974: Extraterrestrial solar spectrum, 3000–6100 Å at 1-Å intervals. *Appl. Opt.,* **13,** 518–522.